ACS Infectious Diseases

Article

Cite This: ACS Infect. Dis. 2019, 5, 473−483

pubs.acs.org/journal/aidcbc

Development of Fungal Selective Amphiphilic Kanamycin: Cost-Effective Synthesis and Use of Fluorescent Analogs for Mode of Action Investigation

Yagya Prasad Subedi,[†] Paul Roberts,[†] Michelle Grilley,[‡] Jon Y. Takemoto,[‡] and Cheng-Wei Tom Chang*[,†]

[†]Department of Chemistry and Biochemistry, Utah State University, 0300 Old Main Hill, Logan, Utah 84322-0300, United States

[‡]Department of Biology, Utah State University, 5305 Old Main Hill, Logan, Utah 84322-5305, United States

Supporting Information

ABSTRACT: Amphiphilic aminoglycosides have attracted interest due to their novel antifungal activities. A crucial but often neglected factor for drug development in academia is cost of production. Herein is reported a one-step, inexpensive synthesis of amphiphilic alkyl kanamycins constituted with only natural components. The synthetic methodology also enabled the preparation of a series fluorescent amphiphilic aryl kanamycins for direct structure−activity mode of action studies. The lead compounds showed prominent antifungal activities against a panel of fungi, including *Fusarium graminearum*, *Cryptococcus neoformans*, and several *Candida* sp., and also significant antibacterial activities. With fluorescence-based whole cell assays, the aryl amphiphilic kanamycins were observed to permeabilize fungal surface membranes at faster rates than bacterial surface membranes. Also, the antifungal action of the amphiphilic kanamycins was observed to occur in a biphasic mode with an initial fast phase correlated with rapid membrane permeabilization at subminimal inhibitory concentrations and a slower phase membrane permeabilization that elevates the reactive oxygen species production leading to cell death. Inactive hydrophobic amphiphilic kanamycins displayed no membrane permeabilization. The results offer cost-effective methods for producing amphiphilic kanamycins and reveal insights into how nonfungal specific amphiphilic kanamycins can be employed for fungal specific diagnostic and therapeutic applications.

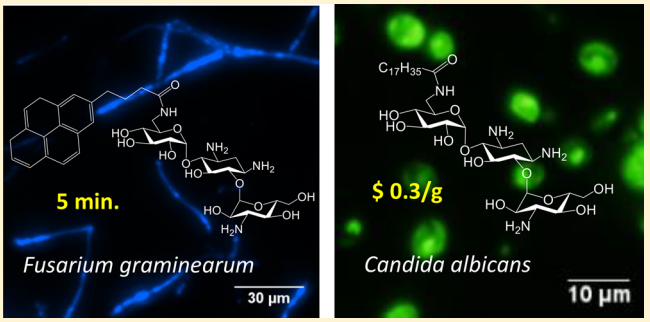

KEYWORDS: *amphiphilic kanamycin, antifungal, agrofungicide, fungal selective, fluorescent kanamycin*

Aminoglycoside antibiotics, once effective against infectious bacterial infections, are plagued with the rampage of antibiotic resistant bacteria.[1] To counteract this problem, modifications of aminoglycoside antibiotics have been studied extensively with the goal of reviving antibacterial activity.[2−5] Recently, the discovery of amphiphilic aminoglycosides provides a new strategy and approach in the fight against resistant bacteria.[6] Unlike traditional aminoglycosides, amphiphilic aminoglycosides have been shown to increase the membrane permeability for both bacteria and fungi.[7−14] The antifungal activity of amphiphilic kanamycin (AK) is of particular interest as it represents a new strategy of repurposing and reviving the use of an old drug.[15−17]

To provide cost-effective antimicrobials, our group has focused on low cost syntheses of AK for uses in green agriculture and human medicine (Figure 1). The lead compound, **K20**, displayed effectiveness in controlling Fusarium head blight in wheat field trials.[18,19] In addition, combinations of **K20** and half-label rates of commonly employed agrofungicides significantly lowered deoxynivalenol (DON) mycotoxin levels in harvested grain. Nevertheless, two shortcomings are associated with **K20**. First, the cost of production of **K20** is not compatible with agrofungicides currently used in the market.[20] Second, **K20** contains a non-natural structural scaffold that makes it difficult to be classified as a natural or organic fungicide. Also, questions still linger regarding the antifungal mode of action of the AKs. Several reports have shown that AKs increase the permeability of fungal membranes.[6−12] However, it is unclear whether this is the sole mode of action (MOA) against fungi. Several studies have reported AKs that are active against both fungi and bacteria (nonfungal specific)[6−10] while **K20** and **FG08** are active only against fungi. Therefore, it is of interest to determine the factors that cause AKs to be fungal or nonfungal specific agents.

RESULTS AND DISCUSSION

Cost-Effective Synthesis of Amphiphilic Kanamycins. To address the cost and natural product issues mentioned

Received: November 23, 2018
Published: January 23, 2019

DOI: 10.1021/acsinfecdis.8b00327
ACS Infect. Dis. 2019, 5, 473−483

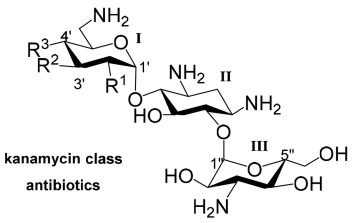

	R^1	R^2	R^3
Kananycin A	OH	OH	OH
Kananycin B	OH	NH_2	OH
Dibekacin	NH_2	H	H
Tobramycin	NH_2	H	OH

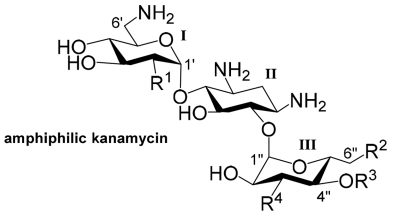

	R^1	R^2	R^3	R^4
K20	OH	$OS(O)_2C_8H_{17}$	H	NH_2
FG08	NH_2	H	C_8H_{17}	OH

Figure 1. Structures of selected kanamycin class antibiotics and AKs.

Scheme 1

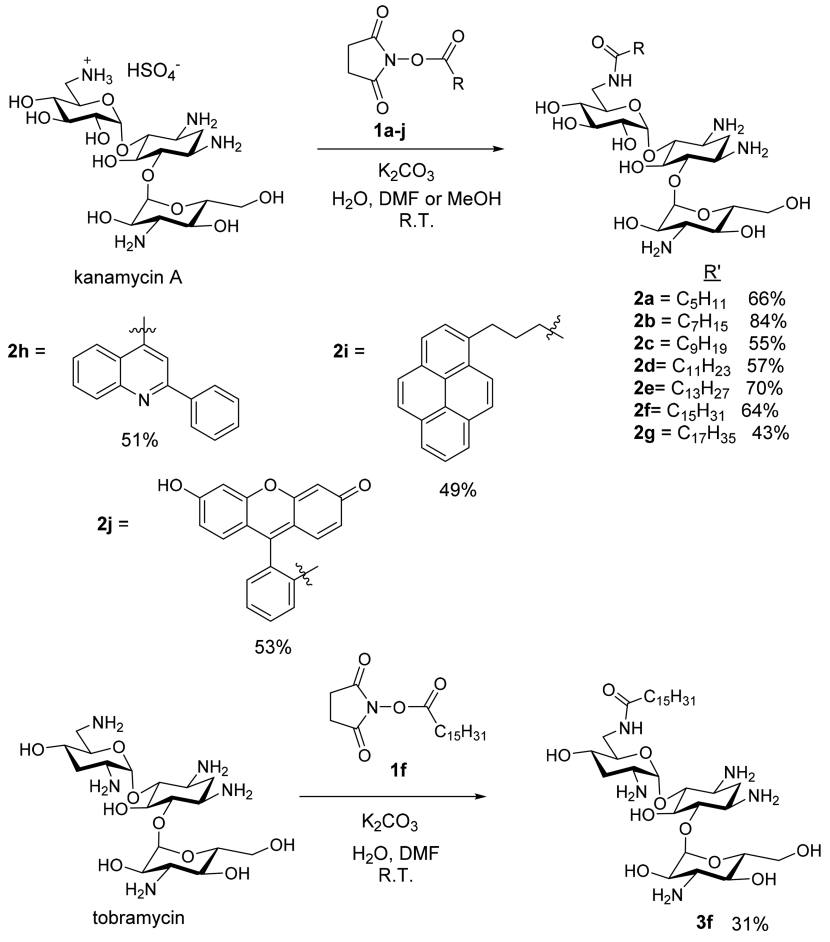

above about AKs, we explored the possibility of AK synthesis in a low cost one-step modification of kanamycin. We selected kanamycin sulfate and fatty acids as the low cost starting materials and attempted one-step regioselective acylation of the amino groups on kanamycin A. The fatty acids were converted into the corresponding esters of *N*-hydroxysuccinimide with modification of a previously reported method.[21] Slow addition of these esters to a solution of kanamycin A afforded the desired AKs (Scheme 1). Modest to excellent yields were achieved for the one-step regioselective acylation. On the basis of the chemicals needed, the cost of production of these AKs is about 1/10 of that for **K20**. Since both fatty acids and kanamycin are natural products, the newly synthesized AKs are anticipated to be classified as natural, thus meeting our goals of price competitiveness and natural and green products. The same synthetic method was used to synthesize **3f** using tobramycin as the starting material. Three derivatives **2h−j** with aryl carboxyl group were also synthesized using the same synthetic methods for potential MOA with direct visualization of time-based uptake in to the fungi, bacteria, and mammalian cell.

Assay of Antifungal and Antibacterial Activities. The newly synthesized AKs were tested for their antibacterial and antifungal activities and cytotoxicity toward mammalian cells. For antifungal activity, a collection of significant human and plant fungal pathogens was used, including *Aspergillus flavus*

DOI: 10.1021/acsinfecdis.8b00327
ACS Infect. Dis. 2019, 5, 473−483

(human and plant pathogen), *Fusarium graminearum* (plant pathogen), *Candida albicans* 64124 (human pathogen, azole resistant), *C. albicans* MYA2876 (human pathogen, azole susceptible), *Cryptococcus neoformans* H99 (human pathogen), and *Rhodotorula pilimanae*, using voriconazole as the controls. From the minimum inhibitory concentrations (MICs), the compounds with linear alkyl chain showed a clear SAR: the antifungal activity increases as the chain length increases (Table 1). The antifungal activity is broad spectrum among various strains which becomes optimal with the attachment of hexadecyl (C16) (**2f** and **3f**) and octadecyl (C18) (**2g**) groups. By comparing the outcomes of **2f** and **3f**, it appears that the core kanamycin is not a significant factor for creating antifungal activity. For AKs with aryl groups, compound **2i** shows the best antifungal activity followed by **2j** whereas **2h** is inactive.

Table 1. MICs of AKs against Fungi[a]

compound	A[b]	B[b]	C[b]	D[b]	E[b]	F[b]
2a	ND[c]	≥256	≥256	≥256	≥256	≥256
2b	ND	≥256	≥256	≥256	≥256	≥256
2c	ND	≥256	≥256	≥256	128	128
2d	256	16	32	32	8	16
2e	256	8	16	16	4	4
2f	32	4	8	8	4	4
2g	16	4	8	8	4	4
2h	ND	≥256	≥256	≥256	128	256
2i	≥256	16	16	16	16	16
2j	≥256	32	64	128	32	16
3f	ND	2	4	4	2	4
K20	32	8	16	16	8	4
FG08	ND	7.8	ND	ND	ND	7.8
kanamycin A	ND	>128	≥256	≥256	≥256	ND
voriconazole	1	32	≥256	0.125	0.125	8

[a]Unit: μg/mL. [b]A: *A. flavus*; B: *F. graminearum* B4-5A; C: *C. albicans* 64124; D: *C. albicans* MYA2876; E: *C. neoformans* H99; F: *R. pilimanae*. [c]ND: not determined.

Since the addition of linear alkyl chain showed superior activities, we selected several of these newly synthesized versions of kanamycin derivatives and investigated their activity against clinically emerging and significant *Candida* species, including *C. albicans* B-311, *C. rugosa* 95-967, *C. parapsolis* Cas08-0490 (azole resistant), and *C. tropicalis* 95-41. *C. albicans* B-311 has been reported to exhibit biotin-independent growth.[22] *C. rugosa* is an emerging human fungal pathogen in some regions with decreased susceptibility to fluconazole, a commonly used antifungal agent.[23] *C. parapsolis* is often the second or most commonly isolated *Candida* species from blood cultures.[24] *C. tropicalis* is the second most virulent *Candida* species found in skin, the gastrointestinal tract, and the female genitourinary tract that is capable of producing biofilm.[25] The MIC values show that the lead compounds are still **2f**, **2g**, and **3f** (Table 2).

Table 2. Minimum Inhibitory Concentration of AKs against *Candida* sp.[a]

compound	A[b]	B[b]	C[b]	D[b]
2c	≥256	≥256	≥256	≥256
2d	128	64	128	128
2e	16	16	32	32
2f	8	8	16	16
2g	8	8	8	16
2i	64	64	128	128
3f	8	8	8	16
K20	16	16	32	32

[a]Unit: μg/mL. [b]A: *C. albicans* B-311; B: *C. rugosa* 95-967; C: *C. parapsolis* Cas08-0490 (azole resistant); D: *C. tropicalis* 95-41.

For the test of antibacterial activity, we selected representative strains of bacteria, including *Escherichia coli* (ATCC 25922), *Staphylococcus aureus* (ATCC 25923), *S. aureus* (ATCC 33591, MRSA), and *S. aureus* (ATCC 43300, MRSA). The AKs with linear alkyl chain showed a similar SAR as their antifungal activity: the antibacterial activity increases as the chain length increases with the most active one bearing hexadecyl or octadecyl groups (Table 3). An interesting difference has been noted: the AKs with octyl groups attached to ring III of kanamycin at the *O*-6″ or *O*-4″ positions, such as **K20** and **FG08**,[11,18] are considered inactive (MICs ≥ 256 μg/mL) against bacteria while exerting noticeable antifungal activity, i.e., fungal specific. In contrast, the attachment of an octyl group at the *N*-6′ position of kanamycin (**2b**) does not manifest either antifungal or antibacterial activity. Comparing the antifungal and antibacterial activities, the bioactivity profile of the newly synthesized AKs appears to resemble those with alkylthio groups at *O*-6″ position.[12] The combined SAR study results reported herein and by others indicate that long linear alkyl groups (C14–C18) are advantageous in exerting antifungal and antibacterial activity, i.e., nonfungal specific. However, these AKs on average show better antifungal activity.

Table 3. MICs of AKs against Bacterial Strains[a]

compound	A[b]	B[b]	C[b]	D[b]
2a	≥256	≥256	≥256	≥256
2b	≥256	≥256	≥256	≥256
2c	≥256	≥256	≥256	≥256
2d	32	32	128	128
2e	64	16	32	32
2f	32	16	16	16
2g	64	32	32	32
2h	≥256	≥256	≥256	≥256
2i	128	32	128	32
2j	128	128	≥256	≥256
3f	32	16	32	32
K20	256	128	>256	>256
FG08	≥256	≥256	ND[c]	ND

[a]Unit: μg/mL. [b]A: *E. coli* (ATCC 25922); B: *S. aureus* (ATCC 25923); C: *S. aureus* (ATCC 33591) MRSA; D: *S. aureus* (ATCC 43300) MRSA. [c]ND: Not determined.

Membrane Permeabilization and Cytotoxicity Study. It has been reported that nonfungal specific AKs cause increases in fungal and bacterial membrane permeabilities.[12,14] Many of these studies were accomplished using fungi treated with AKs with long incubation time (hours). Thus, we were interested in exploring whether nonfungal specific AKs can behave like **K20** or **FG08**, fungal specific AKs, with fast membrane permeabilization properties. We used fluorogenic sytox green dye to investigate the kinetic membrane permeabilization effect of newly synthesized AKs using *C. albicans* MYA2876. The fungi were treated with two AKs, **2b** and **2g**, to observe time-dependent membrane permeabilization. The active **2g** caused a drastic fluorescence increase within minutes, while almost no fluorescence increase was

DOI: 10.1021/acsinfecdis.8b00327
ACS Infect. Dis. 2019, 5, 473−483

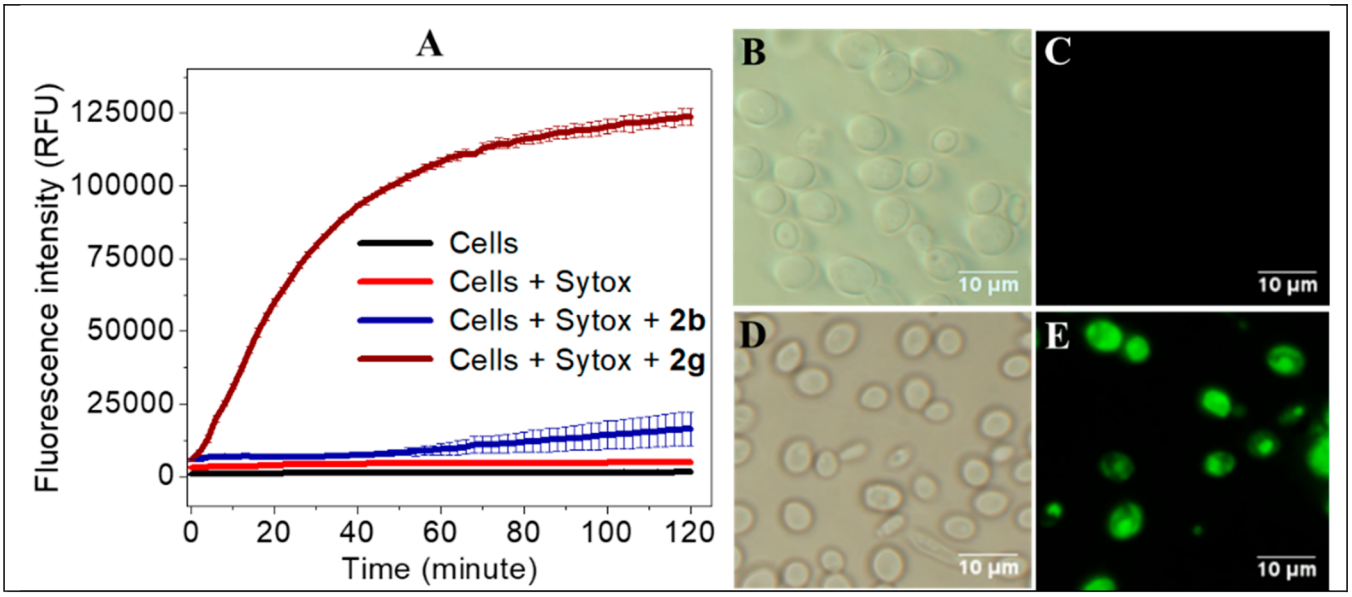

Figure 2. Kinetic membrane permeabilization study of the AKs. (A) Time-dependent measurement of sytox green fluorescence in relative fluorescence unit (RFU); (B, C) images of *C. albicans* MYA2876 treated with **2b** for 60 min; (D, E) images of *C. albicans* MYA2876 treated with **2g** for 60 min.

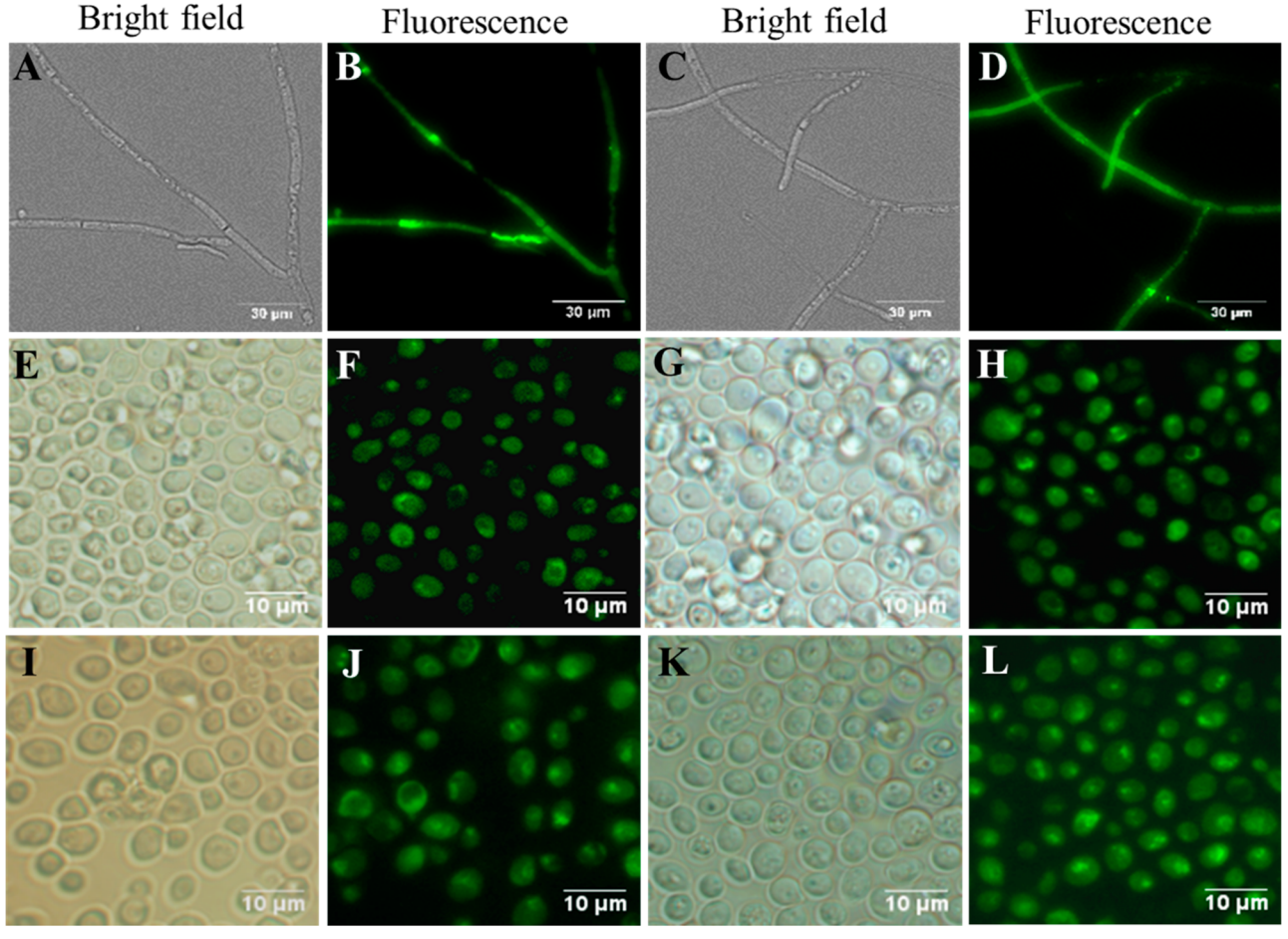

Figure 3. Images of fungi treated with fluorescent **2j**. (A, B) *F. graminearum* treated for 5 min; (C, D) *F. graminearum* treated for 60 min; (E, F) *C. albicans* MYA2876 treated for 5 min; (G, H) *C. albicans* MYA2876 treated for 60 min; (I, J) *C. albicans* 64124 treated for 5 min; (K, L) *C. albicans* 64124 treated for 60 min.

observed for the cells treated with **2b** even after 2 h compared to control (Figure 2). The inability of the **2b** to permeabilize the fungal membrane is consistent with its lack of antifungal activity. This outcome confirms that **2g** causes membrane

DOI: 10.1021/acsinfecdis.8b00327
ACS Infect. Dis. 2019, 5, 473−483

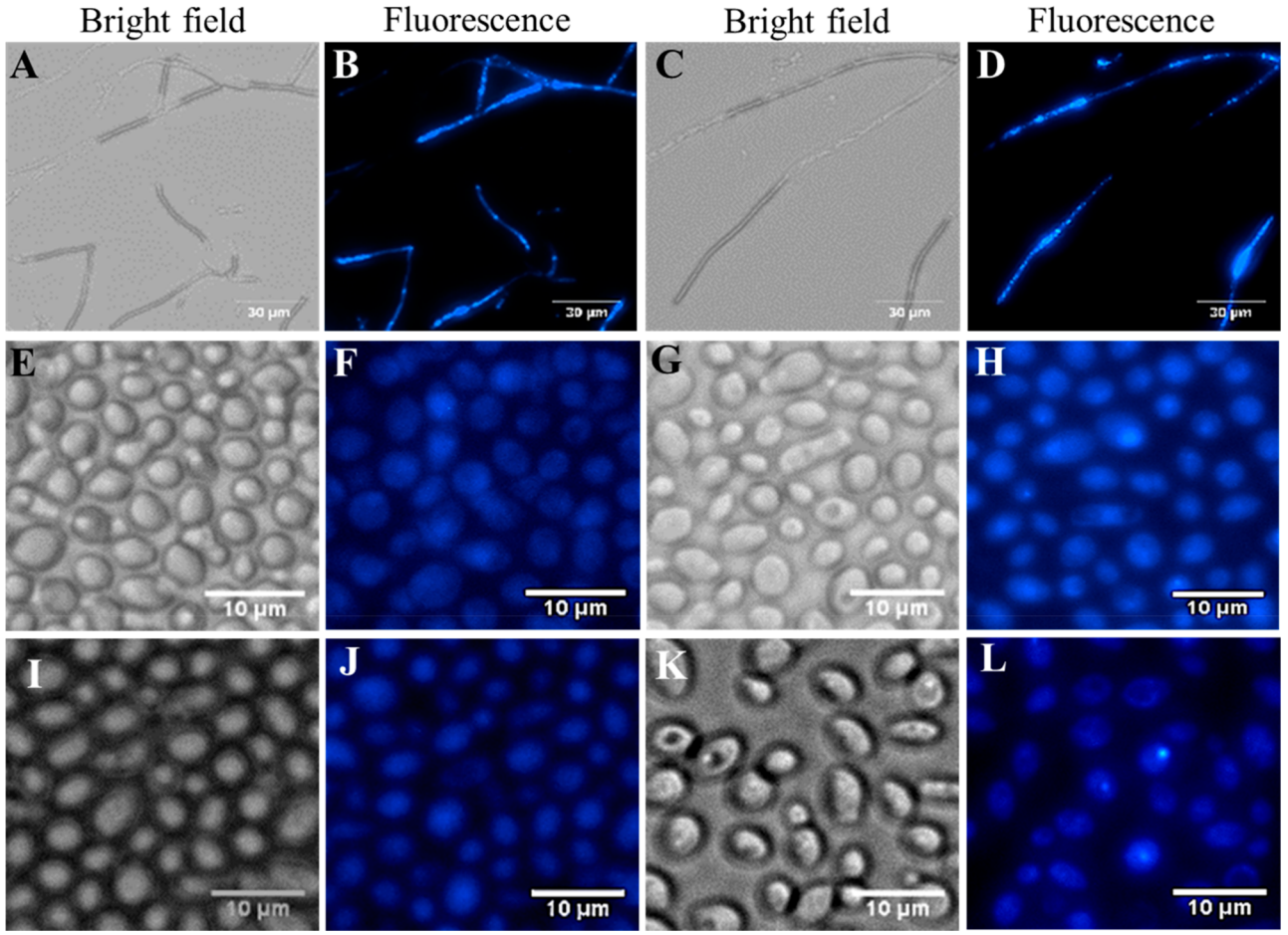

Figure 4. Images of fungi treated with fluorescent **2i**. (A, B) *F. graminearum* treated for 5 min; (C, D) *F. graminearum* treated for 60 min; (E, F) *C. albicans* MYA2876 treated for 5 min; (G, H) *C. albicans* MYA2876 treated for 60 min; (I, J) *C. albicans* 64124 treated for 5 min; (K, L) *C. albicans* 64124 treated for 60 min.

permeabilization consistent with the *fast-acting* nature of **K20** or **FG08** and other membrane permeabilizing agents.

The cytotoxicity (concentration at which 50% of the cells were dead, IC_{50}) of AKs was also determined using HeLa cells.[26] From the IC_{50} values, the cytotoxicity increases as the chain-length of the AKs with linear alkyl group at *N*-6′ position increases where as the typical aminoglycosides in the natural form are reported to be nontoxic up to the 100 μg/mL concentration.[27,28] The result from newly synthesized AKs is consistent with the feature of nonselective membrane targeting antiseptic agents. However, the cytotoxicity for the lead AKs, **2f** and **2g** (IC_{50} of 64.6 and 63.0 μg/mL, respectively), is still *lower* than their antifungal and antibacterial activities. The AKs with aryl (fluorescent) groups and **K20** and **FG08** are considered much less toxic (IC_{50} > 100 μg/mL).

Uptake Study of Amphiphilic Kanamycin Using Fluorescent Analog. To directly observe cell uptake and interaction of the new AKs during membrane permeabilization, AKs (**2h**−**j**) with aryl group were synthesized. However, **2h** was found to be nonfluorescent while **2i** and **2j** show strong fluorescence.[29] Thus, our fluorescence-based investigation was directed to the use of **2i** and **2j**. A recent report showed that AKs incorporated with fluorophores "rapidly accumulated in the cytosol and led to structural changes in proteins and DNA".[30] In the current study, we chose to use hydrophobic fluorophores instead of an alkyl chain/fluorophore combination so that the overall structures of **2i** and **2j** would more closely resemble the amphipathic structural features of the AKs.

First, **2j** was incubated at 32 μg/mL, which is one, 1/4, and 1/2 of the MICs against *F. graminearum*, *C. albicans* MYA2876, and *C. albicans* 64124, respectively (Figure 3). Interestingly, fluorescence from **2j** closely resembled previously reported images[30] and was observed to physically associate with cells of *F. graminearum* and the two *C. albicans* strains *within* 5 min of initial exposure. Therefore, it is likely that AKs not only caused fast membrane permeabilization but also quickly interacted with cells *at concentrations lower than the corresponding MICs*. Incubation for 5 or 60 min revealed preferential localization of **2j** on or in the cells observed as subcellular areas of higher fluorescence intensities. For **2i**, *F. graminearum*, *C. albicans* MYA2876, and *C. ablicans* 64124 were treated with 16 μg/mL, corresponding to their respective MICs (Figure 4). Again, images show a fast (within 5 min) association with cells.

Fluorescent compounds **2i** and **2j** containing aryl group were also investigated for their kinetic membrane permeabilization property using a second fluorescent dye, propidium iodide (PI) (red fluorescence) (Figure 6). *C. albicans* 64124 was treated with **2i** and **2j** at their corresponding MICs (16 μg/mL for **2i** and 64 μg/mL for **2j**). Again, a fast increase of fluorescence from PI was observed when cells were treated with **2i** and **2j** (Figure 5A). The images were taken after 2 h of

DOI: 10.1021/acsinfecdis.8b00327
ACS Infect. Dis. 2019, 5, 473−483

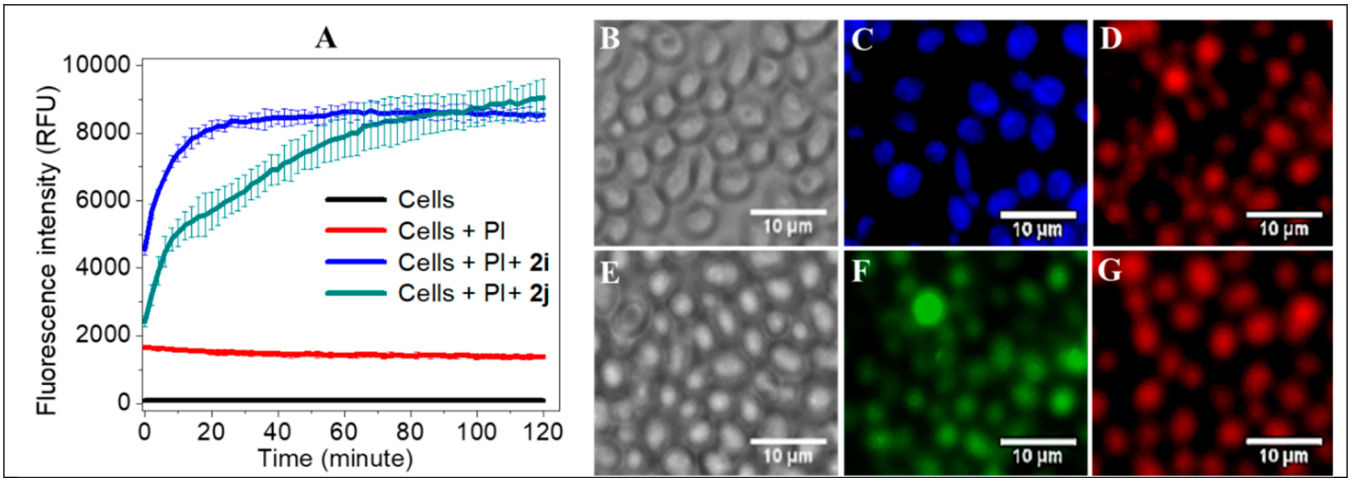

Figure 5. Kinetic membrane permeabilization study of **2i** and **2j** with PI. (A) Time-dependent measurement of fluorescence in relative fluorescence unit (RFU); (B–D) images of *C. albicans* strain 64124 treated with **2i** and PI for 2 h under bright field, blue channel, and red channel; (E–G) images of *C. albicans* strain 64124 treated with **2j** and PI for 2 h under bright field, green channel, and red channel.

incubation and observed in three different fluorescent channels, blue, green, and red, reflecting the presence of **2i**, **2j**, and PI, respectively (Figure 5B–G), along with bright field image. When cells were treated with **2i** and **2j**, fluorescence from all of these compounds can be seen. In contrast, no fluorescence increase was observed when cells were treated with PI alone.[31] Interestingly, the fluorescence profile from treated with **2i** resembles the one treated with **2g** while the fluorescence profile treated with **2j** appears to have two more more phases. The difference may be attributed to the molecular designs: **2i** resembles **2g** more closely as an AK while **2j** has polar functional groups (C═O and OH) on the hydrophobic fluorophore. It is possible that such a structural difference changes the MOA events and kinetics.

To investigate the membrane selectivity of AKs, bacteria (*E. coli* and *S. aureus*) were incubated with **2j** at MIC (128 μg/mL) and 1/4 MIC (32 μg/mL) of both bacteria and the fluorescence was observed after 5 and 60 min of incubation. The images showed that **2j** can still cause membrane permeabilization of bacteria, but higher concentrations (at least at MIC) and longer incubation time are needed.[31] Human cells (HeLa, cervical cancer cells) were incubated with **2j** at 32 μg/mL. No fluorescence was noted after incubation for 5 and 60 min.[31] These results offer useful information on the rate of membrane permeabilization caused by AKs in the order of fungi > bacteria ≫ mammalian cells. This finding, which cannot be revealed by traditional assays such as MIC determination, implies that it is possible to employ AKs for detection or as a diagnostic tool selective toward fungi even though the AKs reported herein and by others show activity against both fungi and bacteria.

Evaluation of Reactive Oxygen Species. Production of cellular reactive oxygen species (ROS) is a common mode of action for antibiotics of various classes.[32] Aminoglycosides are reported as the ROS generator in bacteria and mammalian cells.[28,33,34] Therefore, we decided to examine the production of cellular ROS in fungi treated with the AKs. Four members of the newly synthesized AKs and **K20** were investigated using 2′,7′-dichlorofluorescein diacetate (DCF-DA) dye. Compound **4** (1,1′-(hexane-1,6-diyl)bis(3-decyl-4,9-dioxo-4,9-dihydro-1*H*-naphtho[2,3-*d*][1,2,3]triazol-3-ium triflate)), a cationic anthraquinone analog developed in our group and known to trigger the production of ROS, was used as the positive control.[35,36] DCF-DA dye is nonfluorescent itself and turns into fluorescent 2′,7′-dichlorofluorescein (DCF) once hydrolyzed by the esterage and then oxidized by the ROS species. Incubation of these selected compounds with *C. albicans* MYA2876 reveals that all of the *active* AKs lead to elevated levels of cellular ROS compared to the control having cells only (Figure 6). The

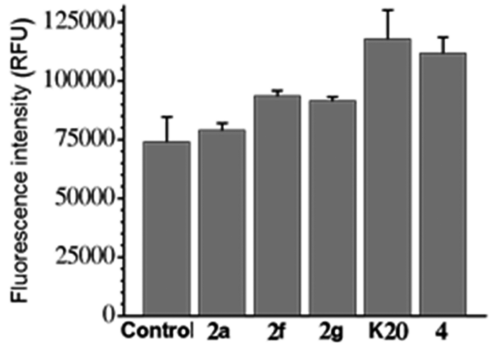

Figure 6. Cellular ROS production.

inactive one, **2b**, has an ROS level similar to the blank control. From the ROS production study, it is reasonable to propose that AKs exert their biological activity by membrane perturbation and then enter the cells causing ROS production, which leads to cascades of cellular oxidative damage and eventual cell death. Particular membrane lipids such as sphingolipids with 4-hydroxylated sphinganine backbones and inositolphosphate-containing head groups that are unique to fungi may play a crucial role in the fungi specific activity of AKs.[13] Therefore, the reason that most of the reported AKs display lower cytotoxicity is likely due to the fact that these AKs simply cannot penetrate the mammalian plasma membrane as quickly as they do with bacterial or fungal membranes.

■ CONCLUSION

We have developed a one-step cost-effective synthesis of a library of AKs from kanamycin. Compared to the common agrofungicides used in agriculture, the cost of production for

DOI: 10.1021/acsinfecdis.8b00327
ACS Infect. Dis. 2019, 5, 473–483

the lead compounds consisting of only natural components is competitive or even lower. The revealed SAR indicates that a long linear alkyl chain (C14−C18) is crucial to generate significant antifungal and antibacterial activities. The analysis of antifungal activity provides a characteristic profile for nonselective membrane-targeting agents. The lead AKs also exhibit minimal cytotoxicity against mammalian cells. From the kinetic membrane permeabilization and fluorescence imaging studies, we discover that, *even for nonfungal specific AKs*, it is possible to achieve fungi selective membrane permeabilization by controlling the time of incubation and concentration of AKs and thus avoid inducing bacterial resistance. Once the integrity of the microbial membrane is compromised, the fast acting AKs can enter the cells, leading to the production of ROS and cell death disrupting the functions of multiple cellular targets. The design of fluorescent AKs that closely resemble the structural features of nonfluorescent AKs provides direct visualization of AKs in action and represents a sensitive and selective diagnostic tool for fungi.

EXPERIMENTAL SECTION

Materials and Methods. Chemicals were purchased from the commercial sources and used without further purification. The fluorescence profile of the compounds was measured in a Spectro fluorophotometer (Shimadzu, RF-5301PC), and fluorescence intensity for the membrane permeabilization study was measured in a Cytation 5 imaging reader. Fluorescence images of the fungi were taken on an Olympus IX innervated fluorescence microscope and Cytation 5 imaging reader. ^{1}H NMR and ^{13}C NMR of the compounds were recorded in Bruker AvanceIII HD Ascend-500 at 283 K temperature.

General Procedure for the Synthesis of 2a−2c. 0.582 g (1 equiv, 1 mmol) of kanamycin sulfate was dissolved in 10 mL of water, and 2 equiv of potassium carbonate was added; the mixture was stirred for 15 min. Then, 1.5 equiv, 1.5 mmol, of NHS-acyl ester dissolved in 10 mL of MeOH was added in 4 portions at a 1 h interval. After 24 h of reaction, solvent was removed by air blowing, and the compound was purified by column chromatography using methanol to 10% NH_4OH in MeOH. Pure compounds in neutral form were acidified with 5% acetic acid and then air blown to dryness. The compound with acetate counterion was passed through the IR410 ion-exchange resin (in Cl^- form) to get the compound with chloride counteranions.

General Procedure for the Synthesis of 2d−2j. 0.582 g (1 equiv, 1 mmol) of kanamycin and 3 equiv of potassium carbonate were dissolved in 10 mL of water; then, 2 equiv of NHS-acyl ester dissolved in 10 mL of DMF was added in 4 portions at a 1 h interval. After 48 h of reaction, solvent was removed by the air blowing, and the compound was purified by column chromatography using MeOH to 10% NH_4OH in MeOH. These compounds were also converted to the cationic form and chloride similar to the compounds **2a−2c**.

6′-*N*-Hexanoylkanamycin A (2a). This compound was synthesized as orange solid by the reaction of kanamycin A sulfate with NHS-hexyl ester, synthesized as before,[37] following the general procedure. ^{1}H NMR (500 MHz, D_2O) δ 5.38 (d, J = 4.0 Hz, 1H), 5.04 (d, J = 3.5 Hz, 1H), 3.8−3.9 (m, 3H), 3.6−3.8 (m, 7H), 3.4−3.6 (m, 6H), 3.24 (t, J = 9.0 Hz, 1H), 2.4−2.5 (m, 1H), 2.20 (t, J = 7.0 Hz, 2H), 1.8−1.9 (m, 1H), 1.4−1.6 (m, 2H), 1.1−1.3 (m, 4H), 0.79 (t, J = 7.0 Hz, 3H); ^{13}C NMR (125 MHz, D_2O) δ 178.04, 100.44, 97.94, 83.55, 79.25, 72.92, 72.73, 72.12, 71.28, 71.10, 70.10, 68.15, 65.34, 59.74, 54.99, 49.70, 48.23, 39.10, 35.73, 30.47, 27.68, 25.12, 21.65, 13.24. ESI/APCI calcd for $C_{24}H_{47}N_4O_{12}^+$ $[MH]^+$: 583.3190; measured m/e: 583.3192.

6′-*N*-Octanoylkanamycin A (2b). This compound was synthesized as white solid by the reaction of kanamycin A sulfate with NHS-octyl ester, synthesized as before,[38] following the general procedure. ^{1}H NMR (500 MHz, D_2O) δ 5.38 (d, J = 4.0 Hz, 1H), 5.04 (d, J = 3.5 Hz, 1H), 3.8−3.9 (m, 3H), 3.6−3.8 (m, 7H), 3.4−3.6 (m, 6H), 3.24 (t, J = 9.5 Hz, 1H), 2.4−2.5 (m, 1H), 2.20 (t, J = 7.5 Hz, 2H), 1.8−1.9 (m, 1H), 1.4−1.6 (m, 2H), 1.1−1.3 (m, 8H), 0.78 (t, J = 7.0 Hz, 3H); ^{13}C NMR (125 MHz, D_2O) δ 178.03, 100.45, 98.03, 83.62, 79.44, 73.00, 72.72, 72.15, 71.27, 71.14, 70.09, 68.16, 65.33, 59.72, 54.99, 49.73, 48.26, 39.06, 35.76, 30.98, 28.11, 28.04, 27.85, 25.41, 21.94, 13.37. ESI/APCI calcd for $C_{26}H_{51}N_4O_{12}^+$ $[MH]^+$: 611.3503; measured m/e: 611.3484.

6′-*N*-Decanoylkanamycin A (2c). This compound was synthesized as white solid by the reaction of kanamycin A sulfate with NHS-decyl ester, synthesized as before,[38] following the general procedure. ^{1}H NMR (500 MHz, D_2O) δ 5.38 (d, J = 4.0 Hz, 1H), 5.04 (d, J = 3.5 Hz, 1H), 3.8−3.9 (m, 3H), 3.6−3.8 (m, 7H), 3.4−3.6 (m, 6H), 3.24 (t, J = 9.5 Hz, 1H), 2.4−2.5 (m, 1H), 2.20 (t, J = 7.5 Hz, 2H), 1.8−1.9 (m, 1H), 1.4−1.6 (m, 2H), 1.1−1.3 (m, 12H), 0.78 (t, J = 7.0 Hz, 3H); ^{13}C NMR (125 MHz, D_2O) δ 178.04, 100.45, 98.07, 83.62, 79.47, 73.02, 72.72, 72.16, 71.26, 71.14, 70.09, 68.16, 65.32, 59.71, 54.99, 49.73, 48.26, 39.07, 35.75, 31.12, 28.60, 28.39, 28.34, 28.14, 27.86, 25.40, 22.04, 13.41. ESI/APCI calcd for $C_{28}H_{55}N_4O_{12}^+$ $[MH]^+$: 639.3816; measured m/e: 639.3788.

6′-*N*-Dodecanoylkanamycin A (2d). This compound was synthesized as white solid by the reaction of kanamycin A sulfate with NHS-dodecyl ester, synthesized as before,[38] following the general procedure. ^{1}H NMR (500 MHz, CD_3OD) δ 5.37 (d, J = 3.5 Hz, 1H), 5.17 (d, J = 4.0 Hz, 1H), 3.8−3.9 (m, 4H), 3.6−3.8 (m, 5H), 3.5−3.6 (m, 5H), 3.4−3.5 (m, 2H), 3.18 (t, J = 9.5 Hz, 1H), 2.5−2.6 (m, 1H), 2.26 (t, J = 7.5 Hz, 2H), 1.9−2.0 (m, 1H), 1.6−1.7 (m, 2H), 1.3−1.4 (m, 16H), 0.92 (t, J = 7.0 Hz, 3H); ^{13}C NMR (125 MHz, CD_3OD) δ 175.81, 99.98, 97.53, 84.11, 80.94, 73.69, 72.91, 72.25, 72.05, 71.71, 71.15, 68.78, 66.18, 60.44, 55.54, 49.87 (one carbon is underneath the solvent peak), 39.39, 35.71, 31.67, 29.39, 29.35, 29.28, 29.15, 29.07, 29.02, 28.26, 25.68, 22.33, 13.05. ESI/APCI calcd for $C_{30}H_{59}N_4O_{12}^+$ $[MH]^+$: 667.4124; measured m/e: 667.4108.

6′-*N*-Tetradecanoylkanamycin A (2e). This compound was synthesized as white solid by the reaction of kanamycin A sulfate with NHS-tetradecyl ester, synthesized as before,[38] following the general procedure. ^{1}H NMR (500 MHz, CD_3OD) δ 5.32 (d, J = 4.0 Hz, 1H), 5.15 (d, J = 4.0 Hz, 1H), 3.8−4.0 (m, 5H), 3.6−3.7 (m, 4H), 3.4−3.6 (m, 7H), 3.18 (t, J = 9.5 Hz, 1H), 2.4−2.5 (m, 1H), 2.25 (t, J = 7.5 Hz, 2H), 1.8−1.9 (m, 1H), 1.6−1.7 (m, 2H), 1.3−1.4 (m, 20H), 0.92 (t, J = 7.0 Hz, 3H); ^{13}C NMR (125 MHz, CD_3OD) δ 175.77, 99.91, 98.01, 84.47, 81.93, 73.61, 72.98, 72.43, 72.10, 71.67, 71.21, 68.84, 66.18, 60.37, 55.58, 49.95 (one carbon is underneath the solvent peak), 39.98, 35.68, 31.67, 29.40, 29.38 (3C), 29.36, 29.27, 29.14, 29.07, 29.01, 25.65, 22.32, 13.03. ESI/APCI calcd for $C_{32}H_{63}N_4O_{12}^+$ $[MH]^+$: 695.4442; measured m/e: 695.4418.

6′-*N*-Hexadecanoylkanamycin A (2f). This compound was synthesized as white solid by the reaction of kanamycin A sulfate with NHS-hexadecyl ester, synthesized as before,[38]

DOI: 10.1021/acsinfecdis.8b00327
ACS Infect. Dis. 2019, 5, 473−483

following the general procedure. ^{1}H NMR (500 MHz, CD_3OD) δ 5.34 (d, J = 3.5 Hz, 1H), 5.17 (d, J = 3.5 Hz, 1H), 3.8−4.0 (m, 5H), 3.6−3.8 (m, 4H), 3.4−3.6 (m, 7H), 3.18 (t, J = 9.5 Hz, 1H), 2.4−2.6 (m, 1H), 2.25 (t, J = 7.5 Hz, 2H), 1.8−1.9 (m, 1H), 1.6−1.7 (m, 2H), 1.3−1.4 (m, 24H), 0.92 (t, J = 7.0 Hz, 3H); ^{13}C NMR (125 MHz, CD_3OD) δ 175.78, 99.92, 97.75, 84.28, 81.41, 73.66, 72.97, 72.30, 72.05, 71.68, 71.19, 68.82, 66.17, 60.37, 55.55, 49.88 (one carbon is underneath the solvent peak), 39.97, 35.68, 31.67, 29.40, 29.38 (5C), 29.36, 29.27, 29.14, 29.07, 29.01, 25.65, 22.32, 13.03. ESI/APCI calcd for $C_{32}H_{63}N_4O_{12}^+$ $[MH]^+$: 723.4755; measured m/e: 723.4750.

6′-*N*-Octadecanoylkanamycin A (2g). This compound was synthesized as white solid by the reaction of kanamycin A sulfate with NHS-octadecyl ester, synthesized as before,[38] following the general procedure. ^{1}H NMR (500 MHz, CD_3OD) δ 5.33 (d, J = 4.0 Hz, 1H), 5.15 (d, J = 3.5 Hz, 1H), 3.8−4.0 (m, 5H), 3.6−3.8 (m, 4H), 3.4−3.6 (m, 7H), 3.18 (t, J = 9.5 Hz, 1H), 2.4−2.6 (m, 1H), 2.26 (t, J = 7.0 Hz, 2H), 1.8−1.9 (m, 1H), 1.6−1.7 (m, 2H), 1.3−1.4 (m, 28H), 0.92 (t, J = 7.0 Hz, 3H); ^{13}C NMR (125 MHz, CD_3OD) δ 175.77, 99.93, 98.00, 84.44, 81.90, 73.61, 72.97, 72.44, 72.10, 71.69, 71.20, 68.84, 66.18, 60.38, 55.58, 49.96 (one carbon is underneath the solvent peak), 39.97, 35.68, 31.67, 29.39 (7C), 29.35, 29.35, 29.29, 29.15, 29.07, 29.02, 25.66, 22.33, 13.04. ESI/APCI calcd for $C_{36}H_{71}N_4O_{12}^+$ $[MH]^+$: 751.5063; measured m/e: 751.5057.

6′-*N*-(2-Phenyl-4-quinolinecarbonyl)kanamycin A (2h). To 2.49 g (1 equiv, 10 mmol) of 2-phenylquinoline-4-carboxylic acid dissolved in 50 mL of anhydrous DMF were added 1.725 g (1.5 equiv, 30 mmol) of *N*-hydroxysuccinimide and 4.125 g (2 equiv, 40 mmol) of *N*,*N*′-dicyclohexylcarbodiimide, and the solution was stirred overnight at room temperature. After filtration of the reaction mixture, the solvent from the filtrate was removed by air blowing. The residue was recrystallized from dichloromethane and ether to obtain pure 2,5-dioxopyrrolidin-1-yl 2-phenylquinoline-4-carboxylate (**1h**) with 78% yield. ^{1}H NMR (500 MHz, $CDCl_3$) δ 8.67 (dt, J = 8.5, Hz, 1H), 8.6 (s, 1H), 7.59 (s, 1H), 8.30 (s, J = 8.5 Hz, 1H), 8.24 (d, J = 7.5 Hz, 2H) 7.85 (dt, J = 7.5, 1.5 Hz, 1H), 7.70 (dt, J = 7.5, 1.5 Hz, 1H) 7.5−7.6 (m, 3H), 3.00 (s, 4H); ^{13}C NMR (125 MHz, $CDCl_3$) δ 168.92 (2C), 161.57, 156.64, 148.91, 137.97, 131.06, 130.70, 130.37, 130.19, 129.07 (2C), 128.74, 127.63 (2C), 124.90, 123.42, 121.05, 25.78 (2C). ESI/APCI calcd for $C_{20}H_{15}N_2O_4^+$ $[MH]^+$: 347.1032; measured m/e: 347.1016. Kanamycin A sulfate was reacted with 2,5-dioxopyrrolidin-1-yl 2-phenylquinoline-4-carboxylate as described in the general procedure to give the white solid 6′-*N*-(2-phenyl-4-quinolinecarbonyl)kanamycin A. ^{1}H NMR (500 MHz, D_2O) δ 7.82 (t, J = 8.0 Hz, 2H), 7.6−7.7 (m, 3H), 7.59 (s, 1H), 7.47 (t, J = 8.0 Hz, 1H), 7.3−7.4 (m, 3H), 5.22 (d, J = 3.5 Hz, 1H), 4.29 (d, J = 3.5 Hz, 1H), 4.05 (dd, J = 14.0 Hz, J = 3.5 Hz, 1H), 3.8−3.9 (m, 1H), 3.7−3.8 (m, 3H), 3.3−3.4 (m, 7H), 3.2−3.3 (m, 2H), 3.15 (t, J = 11.0 Hz, 1H), 2.99 (t, J = 10.0 Hz, 1H), 2.3−2.4 (m, 1H), 2.2−2.3 (m, 1H) 1.7−1.8 (m, 1H); ^{13}C NMR (125 MHz, D_2O) δ 169.49, 157.13, 147.25, 142.75, 137.51, 131.07, 130.22, 129.06 (2C), 127.95, 127.88, 127.56 (2C), 124.77, 122.83, 117.68, 98.66, 95.04, 83.71, 78.31, 72.58, 72.45, 71.51, 71.03, 71.02, 70.97, 67.67, 65.89, 59.74, 54.68, 48.94, 47.36, 40.43, 27.70. ESI/APCI calcd for $C_{34}H_{46}N_5O_{12}^+$ $[MH]^+$: 716.3143; measured m/e: 716.3107.

6′-*N*-(1-Pyrenebutanoyl)kanamycin A (2i). This compound was synthesized as white solid by the reaction of kanamycin A sulfate with 2,5-dioxopyrrolidin-1-yl 4-(pyren-1-yl)butanoate, synthesized as before,[39] following the general procedure. ^{1}H NMR (500 MHz, D_2O) δ 7.98 (d, J = 7.5 Hz, 1H), 7.95 (d, J = 7.5 Hz, 1H), 7.7−7.9 (m, 6H), 7.55 (d, J = 7.5 Hz, 1H), 4.91 (d, J = 3.5 Hz, 1H), 4.77 (d, J = 3.5 Hz, 1H), 3.6−3.8 (m, 4H), 3.4−3.6 (m, 6H), 3.3−3.4 (m, 4H), 2.9−3.2 (m, 5H), 2.3−2.4 (m, 1H), 2.1−2.3 (m, 2H), 1.9−2.0 (m, 2H), 1.6−1.8 (m, 2H); ^{13}C NMR (125 MHz, D_2O) δ 176.86, 135.64, 130.83, 130.32, 129.18, 127.96, 127.35, 127.12, 126.95, 126.33, 126.06, 124.79, 124.74, 124.67, 123.89, 123.86, 123.02, 100.31, 96.93, 83.47, 78.68, 72.69, 72.31, 72.14, 70.98, 70.90, 70.43, 67.99, 65.24, 59.67, 54.96, 49.53, 47.85, 39.47, 35.19, 31.31, 27.48, 26.58. ESI/APCI calcd for $C_{38}H_{51}N_4O_{12}^+$ $[MH]^+$: 755.3503; measured m/e: 755.3476.

6′-*N*-(Fluorescein)kanamycin A (2j). This compound was synthesized as white solid by the reaction of kanamycin A sulfate with 2,5-dioxopyrrolidin-1-yl 2-(6-hydroxy-3-oxo-3*H*-xanthen-9-yl)benzoate, synthesized as before,[40] following the general procedure. ^{1}H NMR (500 MHz, D_2O) δ 7.77 (d, J = 7.5 Hz, 1H), 7.31 (t, J = 7.0 Hz, 1H), 7.08 (t, J = 7.0 Hz, 1H), 6.63 (s, 1H), 6.57 (s, 1H), 6.39 (d, J = 7.5 Hz, 1H), 6.33 (t, J = 8.5 Hz, 2H), 6.24 (d, J = 9.0 Hz, 1H), 6.18 (d, J = 8.5 Hz, 1H), 5.05 (d, J = 3.5 Hz, 1H) (one proton hidden inside solvent peak), 3.3−3.9 (m, 15H), 2.7−2.9 (m, 2H), 2.4−2.5 (m, 1H), 1.8−1.9 (m, 1H); ^{13}C NMR (125 MHz, D_2O) δ 171.94, 157.26, 156.86, 153.39, 152.72, 152.54, 133.80, 129.92, 129.55, 129.02, 128.85, 123.78, 122.82, 112.47, 111.86, 111.27, 108.99, 102.71, 102.35, 100.61, 98.22, 83.53, 79.54, 73.17, 72.66, 71.18, 71.08, 70.51, 69.87, 68.18, 66.20, 65.23, 59.60, 55.03, 49.77, 48.47, 41.28, 27.28. ESI/APCI calcd for $C_{38}H_{47}N_4O_{15}^+$ $[MH]^+$: 799.3032; measured m/e: 799.3037.

6′-*N*-Hexadecanoyltobramycin (3f). 0.20 g (1 equiv, 0.50 mmol) of tobramycin and 2 equiv of potassium carbonate were dissolved in 10 mL of water; then, 2 equiv of NHS-hexadecyl ester, as synthesized before,[38] in 10 mL of DMF was added in 4 portions at a 1 h interval. After 48 h of reaction, solvent was removed by air blowing and the compounds was purified by column chromatography using 100% MeOH to 10% NH_4OH in MeOH.

^{1}H NMR (500 MHz, D_2O) δ 5.38 (d, J = 4.0 Hz, 1H), 5.04 (d, J = 3.5 Hz, 1H), 3.8−3.9 (m, 3H), 3.6−3.8 (m, 7H), 3.4−3.6 (m, 6H), 3.24 (t, J = 9.0 Hz, 1H), 2.4−2.5 (m, 1H), 2.20 (t, J = 7.0 Hz, 2H), 1.8−1.9 (m, 1H), 1.4−1.6 (m, 2H), 1.1−1.3 (m, 4H), 0.79 (t, J = 7.0 Hz, 3H); ^{13}C NMR (125 MHz, D_2O) δ 178.04, 100.44, 97.94, 83.55, 79.25, 72.92, 72.73, 72.12, 71.28, 71.10, 70.10, 68.15, 65.34,59.74, 54.99, 49.70, 48.23, 39.10, 35.73, 30.47, 27.68, 25.12, 21.65, 13.24. ESI/APCI calcd for $C_{34}H_{68}N_5O_{10}^+$ $[MH]^+$: 706.4966; measured m/e: 706.4975.

Procedure for Antibacterial Assay. Antibacterial activity of the compounds was tested against *E. coli* (ATCC25922), *S. aureus* (ATCC25923), *S. aureus* MRSA (ATCC 33591), and *S. aureus* MRSA (ATCC 43300). Bacteria were grown in Lysogeny broth (LB) medium at 35 °C for 18 h before using for the assay. The compounds (50 μL) with concentrations from 512 to 0.25 μg/mL with 2-fold dilution were added in a 96 well plate. Then, 50 μL of bacterial growth with scattering OD_{600} adjusted from 0.08 to 0.1 was added to each well with the solution of the compounds and incubated at 35 °C for 18 h. Then, the minimum concentration of the compounds which inhibits the growth of the bacteria to the visible clearance was

DOI: 10.1021/acsinfecdis.8b00327
ACS Infect. Dis. 2019, 5, 473−483

recorded as the minimum inhibitory concentration of the compound.

Procedure for Antifungal Assay. Antifungal activity of the synthesized compounds was tested against *Aspergillus flavus* (human and plant pathogen), *Fusarium graminearum* B4-5A (plant pathogen), *Candida albicans* 64124 (human pathogen, azole resistant), *C. albicans* MYA2876 (human pathogen, azole susceptible), *Cryptococcus neoformans* H99 (human pathogen), and *Rhodotorula pilimanae*, using voriconazole as the control following the standard protocol.[41,42] RPMI 1640 medium supplemented with 0.165 M 3-(*N*-morpholino)propanesulfonic acid (MOPS; pH = 7.0) was used for growing the fungi and during the assay of the compounds. For *Fusarium*, 1×10^5 cells/mL and, for other fungal strains, 2×10^4 cells/mL cell confluence were used during the assay of the compounds. The fungal cells were treated with the compounds from 256 to 0.125 μg/mL with 2-fold dilution in a 96 well plate and incubated for 24 to 36 h. The concentration of the compounds which inhibited the growth of the compounds to clearance was considered as the minimum concentration of the compounds.

Procedure for Membrane Permeabilization Study of 2b and 2g. *Candida albicans* MYA2876 cells were grown in potato dextrose broth (PDB) at 28 °C for 48 h. Cells were spun down at 10 000 rpm for 2 min in a Fisher Scientific accuSpin Micro centrifuge at room temperature and resuspended in water. Controls (cells only and cells treated with sytox green) along with cells treated with **2b**, **2g**, and sytox green in water were added to different wells of 96 well plates (Costar 3925), maintaining a final volume of 200 μL and cell confluence of 1×10^7 cells/mL. The final concentrations of **2b** and **2g** were 8 μg/mL, and the final concentration of sytox was 0.125 μM. Fluorescent intensity was measured every 2 min for 2 h with excitation wavelength of 485 nm and emission wavelength of 528 nm in a Cytation 5 imaging reader. The experiment was performed in triplicate. In this study, the fluorescence intensity at 60 min was similar to the fluorescence at 2 h, especially for the active compound **2g**, so we did the imaging of the cells treated with the compounds for 60 min in the bright field and green channels.

Procedure for Kinetic Membrane Permeabilization Study of 2i and 2j. The excitation and emission wavelengths of **2j** overlapped with the sytox green dye used in the membrane permeabilization study of **2a** and **2g**. Therefore, we used propidium iodide (PI), a red fluorescence dye, in this study. Propidium iodide functions in the same way as sytox green, with no or less fluorescence by itself (Figure 4) and an increase in fluorescence upon binding to the nucleic acids (reported in the manuscript). *Candida albicans* 64124 grown in PDB medium was washed with water and treated with **2i** and **2j** in water maintaining a final concentration of compounds of 1× MIC (16 μg/mL for **2i** and 64 μg/mL for **2j**) and propidium iodide of 2 μg/mL. Fluorescence intensity was measured every 2 min for 2 h in a Cytation 5 imaging reader with excitation wavelength of 538 nm and emission wavelength of 617 nm. From this study, we see the increase in fluorescence up to 2 h, especially for **2j**, so we did the imaging of the cells incubated for 2 h in the bright field and blue and red channels.

Procedure for the Fluorescence Imaging of Fungi. *Fusarium graminerum* spores (1×10^5) were grown in PDB medium at 28 °C for 18 h with gentle shaking. One mL of fungi growth was washed twice with water by spinning down at 13 000 rpm for 5 min in a Fisher Scientific accuSpin Micro centrifuge at room temperature and resuspended in 500 μL of water. Then, **2i** and **2j** were added to the fungi (16 μg/mL for **2i** and 32 μg/mL for **2j**) and incubated at 37 °C for 5 and 60 min. After incubation, the cells were washed two times and resuspended in water. Images were taken in blue (for **2i**) and green (for **2j**) channels in a Cyatation 5 imaging reader using a 40× objective. Similarly, *C. albicans* 64124 and *C. albicans* MYA were grown in PDB medium for 48 h at 28 °C with gentle shaking. One mL of growth was washed with water twice by spinning down at 10 000 rpm for 2 min in a Fisher Scientific accuSpin Micro centrifuge at room temperature and resuspended in the same volume of water. Then, the cells were treated with 16 μg/mL of **2i** and 32 μg/mL of **2j** in water maintaining the cell confluence at 1×10^7 in 1 mL and incubated at 37 °C for 5 and 60 min. After incubation, cells were washed with water two times and resuspended in the same volume of water. The images of fungi treated with **2i** were taken in a Cyation 5 imaging reader in a blue channel using a 40× objective, and the images of the **2j** were taken in an Olympus IX71 microscope in the green channel using a 100× oil immersion objective.

Procedure for the Assay of Reactive Oxygen Species (ROS) Generation. *Candida albicans* MYA grown in potato dextrose broth (PDB) medium was washed with water and then treated with 1× MIC of **2f**, **2g**, **2i**, **K20**, and **4** (Figure 3) (8 μg/mL for **2f** and **2g**, 16 μg/mL for **2i** and **K20**, and 4 μg/mL for compound **4**), 16 μg/mL of **2b**, and only media (control) in RPMI1640 and incubated for 3 h at 37 °C. Compound **4**, known to produce reactive oxygen species, was used as the positive control.[31,32] After incubation with compounds, cells were washed with water twice, and then, 25 μM of DCF-DA dye dissolved in RPMI medium was added and incubated for another 30 min at 37 °C. Then, the cells were washed with water twice, and the fluorescence intensity of the cells was measured in a Cytation 5 imaging reader with excitation wavelength of 485 nm and emission wavelength of 525 nm.

■ ASSOCIATED CONTENT

Supporting Information

The Supporting Information is available free of charge on the ACS Publications website at DOI: 10.1021/acsinfecdis.8b00327.

Excitation and emission fluorescent spectra of **2i** and **2j**, images of HeLa cells and bacteria with **2j**, cytotoxicity of the compounds toward HeLa cells, and ^{1}H NMR, ^{13}C NMR, and ^{1}H−^{1}H COSY spectra of the compounds (PDF)

■ AUTHOR INFORMATION

Corresponding Author

*E-mail: tom.chang@usu.edu.

ORCID

Cheng-Wei Tom Chang: 0000-0002-8978-4520

Notes

The authors declare no competing financial interest.

■ ACKNOWLEDGMENTS

We acknowledge the support from the Department of Chemistry and Biochemistry, Utah State University. This work was supported in part by NSF Award CHE-1429195 for a

DOI: 10.1021/acsinfecdis.8b00327
ACS Infect. Dis. 2019, 5, 473−483

500 MHz Bruker NMR and by grants from the Utah Science, Technology and Research (USTAR) initiative and USDA-National Institute of Food and Agriculture (UTA01271). We thank Prof. Gary Yuen of University of Nebraska and Mr. Michael Miller of Baicor, L.C. for assistance in cost estimates for agrofungicide use and production.

DEDICATION

This publication is dedicated to Dr. Gene W. Miller (1925−2017) whose generous support sparked the growing research on antifungal amphiphilic aminoglycosides.

ABBREVIATIONS

AK, amphiphilic kanamycin; DCF-DA, 2′,7′-dichlorofluorescein diacetate; DCF, 2′,7′-dichlorofluorescein; IC_{50}, concentration at which 50% of the cells were dead; LB, Lysogeny broth; PDB, potato dextrose broth; MIC, minimum inhibitory concentration; MOPS, 3-(*N*-morpholino)propanesulfonic acid; MTT, 3-(4,5-dimethylthiazol-2-yl)-2,5-diphenyltetrazolium bromide; PI, propidium iodide; ROS, reactive oxygen species

REFERENCES

(1) Umezawa, S., and Tsuchiya, T. (1982) In *Aminoglycoside Antibiotics* (Umezawa, H., and Hooper, L. R., Eds.), pp 37−110, Springer-Verlag, New York.

(2) Haddad, J., Kotra, L. P., and Mobashery, S. (2001) In *Glycochemistry Principles, Synthesis, and Applications* (Wang, P. G., and Bertozzi, C. R., Eds.), pp 353−424, Marcel Dekker, Inc., New York/Basel.

(3) Wang, J., and Chang, C.-W. T. (2007) In *Aminoglycoside Antibiotics* (Arya, D. P., Ed.), pp 141−180, John Wiley & Sons, Inc., New York.

(4) Green, K. D., Chen, W., Houghton, J. L., Fridman, M., and Garneau-Tsodikova, S. (2010) Exploring the substrate promiscuity of drug-modifying enzymes for the chemoenzymatic generation of N-acylated aminoglycosides. *ChemBioChem 11*, 119−126.

(5) Chandrika, N. T., and Garneau-Tsodikova, S. (2018) Comprehensive review of chemical strategies for the preparation of new aminoglycosides and their biological activities. *Chem. Soc. Rev. 47*, 1189−1249.

(6) Hanessian, S., Pachamuthu, K., Szychowski, J., Giguere, A., Swayze, E. E., Migawa, M. T., Francois, B., Kondo, J., and Westhof, E. (2010) Structure-based design, synthesis and A-site rRNA co-crystal complexes of novel amphiphilic aminoglycoside antibiotics with new binding modes: a synergistic hydrophobic effect against resistant bacteria. *Bioorg. Med. Chem. Lett. 20*, 7097−7101.

(7) Zhang, J., Chiang, F.-I., Wu, L., Czyryca, P. G., Li, D., and Chang, C.-W. T. (2008) Surprising alteration of antibacterial activity of 5″-modified neomycin against resistant bacteria. *J. Med. Chem. 51*, 7563−7573.

(8) Bera, S., Zhanel, G. G., and Schweizer, F. (2010) Antibacterial activities of aminoglycoside antibiotics-derived cationic amphiphiles. Polyol-modified neomycin B-, kanamycin A-, amikacin-, and neamine-based amphiphiles with potent broad spectrum antibacterial activity. *J. Med. Chem. 53*, 3626−3631.

(9) Ouberai, M., El Garch, F., Bussiere, A., Riou, M., Alsteens, D., Lins, L., Baussanne, I., Dufrêne, Y. F., Brasseur, R., Decout, J.-L., and Mingeot-Leclercq, M.-P. (2011) The Pseudomonas aeruginosa membranes: a target for a new amphiphilic aminoglycoside derivative? *Biochim. Biophys. Acta, Biomembr. 1808*, 1716−1727.

(10) Herzog, I. M., Green, K. D., Berkov-Zrihen, Y., Feldman, M., Vidavski, R. R., Eldar-Boock, A., Satchi-Fainaro, R., Eldar, A., Garneau-Tsodikova, S., and Fridman, M. (2012) 6″-Thioether tobramycin analogues: towards selective targeting of bacterial membranes. *Angew. Chem., Int. Ed. 51*, 5652−5656.

(11) Chang, C.-W. T., Fosso, M. Y., Kawasaki, Y., Shrestha, S. K., Bensaci, M. F., Wang, J., Evans, C. K., and Takemoto, J. Y. (2010) Antibacterial to antifungal conversion of neamine aminoglycosides through alkyl modification. Strategy for reviving old drugs into agrofungicides. *J. Antibiot. 63*, 667.

(12) Fosso, M. Y., Shrestha, S. K., Green, K. D., and Garneau-Tsodikova, S. (2015) Synthesis and bioactivities of kanamycin B derived cationic amphiphiles. *J. Med. Chem. 58*, 9124−9132.

(13) Shrestha, S., Grilley, M., Fosso, M. Y., Chang, C.-W. T., and Takemoto, J. Y. (2013) Membrane lipid-modulated mechanism of action and non-cytotoxicity of novel fungicide aminoglycoside FG08. *PLoS One 8*, e73843.

(14) Steinbuch, K. B., Benhamou, R. I., Levin, L., Stein, R., and Fridman, M. (2018) Increased degree of unsaturation in the lipid of antifungal cationic amphiphiles facilitates selective fungal cell disruption. *ACS Infect. Dis. 4* (5), 825−836.

(15) Subedi, Y. P., AlFindee, M. N., Takemoto, J. Y., and Chang, C.-W. T. (2018) Antifungal amphiphilic kanamycins: new life for an old drug. *MedChemComm 9*, 909−919.

(16) Chang, C.-W. T., and Takemoto, J. Y. (2014) Antifungal amphiphilic aminoglycosides. *MedChemComm 5*, 1048−105.

(17) Chang, C.-W. T., and Takemoto, J. Y. (2014) US Patent 8,865,665.

(18) Shrestha, S. K., Chang, C.-W. T., Meissner, N., Oblad, J., Shrestha, J. P., Sorensen, K. N., Grilley, M. M., and Takemoto, J. Y. (2014) Antifungal amphiphilic aminoglycoside K20: bioactivities and mechanism of action. *Front. Microbiol. 5*, 671.

(19) Takemoto, J. Y., Wegulo, S., Yuen, G. Y., Stevens, J. L., Jochum, C. C., Chang, C.-W. T., Kawasaki, Y., and Miller, G. W. (2018) Suppression of wheat Fusarium head blight by novel amphiphilic aminoglycoside fungicide K20. *Fungal Biol. 122*, 465−470.

(20) The estimated cost for applying **K20** (calculated with chemicals needed for the synthesis alone) is $60/acre while the costs of agrofungicides in the market, such as Caramba, Prosaro SC, and Headline, are $18.7/acre, $17.9/acre, and $16.0/acre, respectively. The cost of **K20** is calculated on the basis of the cost of chemicals for the synthesis and amount used for field spraying as reported in ref 13. The cost for commercial agrofungicides is calculated from the survey of market price reported from the Institute of Agriculture and Natural Resources, University of Nebraska−Lincoln (UNL) (https://cropwatch.unl.edu/2017-CW-News/2017-documents/disease-management/UNL-EC130-Fungicide-Prices-2017.pdf) and the amounts employed for the field spraying as reported in reference 13.

(21) Chandrika, N. T., Green, K. D., Houghton, J. L., and Garneau-Tsodikova, S. (2015) Synthesis and Biological Activity of Mono- and Di-N-acylated Aminoglycosides. *ACS Med. Chem. Lett. 6*, 1134−1139.

(22) Vidotto, V., Pugliese, A., and Gioannini, P. (1987) Growth of Candida albicans in a minimal synthetic medium without biotin. *Mycopathologia 100*, 7−15.

(23) Pfaller, M. A., Diekema, D. J., Colombo, A. L., Kibbler, C., Ng, K. P., Gibbs, D. L., Newell, V. A., and the Global Antifungal Surveillance Group (2006) Candida rugosa, an Emerging Fungal Pathogen with Resistance to Azoles: Geographic and Temporal Trends from the ARTEMIS DISK Antifungal Surveillance Program. *J. Clin, Microbiol. 44*, 3578−3582.

(24) Trofa, D., Gácser, A., and Nosanchuk, J. D. (2008) *Candida parapsilosis*, an emerging fungal pathogen. *Clin. Microbiol. Rev. 21*, 606−625.

(25) Sardi, J. C. O., Scorzoni, L., Bernardi, T., Fusco-Almeida, A. M., and Mendes Giannini, M. J. S. (2013) Candida species: current epidemiology, pathogenicity, biofilm formation, natural antifungal products and new therapeutic options. *J. Med. Microbiol. 62*, 10−24.

(26) Please refer to the Supporting Information for details.

(27) AlFindee, M., Subedi, Y. P., Fiori, M., Krishnan, S., Kjellgren, A., Altenberg, G. A., and Chang, C.-W. T. (2018) Inhibition of Connexin Hemichannels by New Amphiphilic Amino-glycosides without Antibiotic Activity. *ACS Med. Chem. Lett. 9* (7), 697−701.

(28) Cuccarese, M. F., Singh, A., Amiji, M., and O'Doherty, G. A. (2013) A novel use of gentamicin in the ROS-mediated sensitization

DOI: 10.1021/acsinfecdis.8b00327
ACS Infect. Dis. 2019, 5, 473−483

of NCI-H460 lung cancer cells to various anticancer agents. *ACS Chem. Biol. 8* (12), 2771−2777.
(29) Information on fluorescence properties of **2i** and **2j** and other related results can be found in the Supporting Information.
(30) Jaber, Q. Z., Benhamou, R. I., Herzog, I. M., Baruch, B. B., and Fridman, M. (2018) Cationic amphiphiles induce macromolecule denaturation and organelle decomposition in pathogenic yeast. *Angew. Chem., Int. Ed. 57* (50), 16391−16395.
(31) Please refer to the Supporting Information for detailed images.
(32) Kohanski, M. A., Dwyer, D. J., Hayete, B., Lawrence, C. A., and Collins, J. J. (2007) A common mechanism of cellular death induced by bactericidal antibiotics. *Cell 130*, 797−810.
(33) Desa, D. E., Nichols, M. G., and Smith, H. J. (2019) Aminoglycosides rapidly inhibit NAD (P) H metabolism increasing reactive oxygen species and cochlear cell demise. *J. Biomed. Opt. 24* (5), 051403.
(34) Ye, J.-z., Su, Y.-b., Lin, X.-m., Lai, S.-s., Li, W.-x., Ali, F., Zheng, J., and Peng, B. (2018) Alanine enhances aminoglycosides-induced ROS production as revealed by proteomic analysis. *Front. Microbiol. 9*, 29.
(35) Shrestha, J. P., Baker, C., Kawasaki, Y., Subedi, Y. P., Vincent de Paul, N. N., Takemoto, J. Y., and Chang, C.-W. T. (2017) Synthesis and bioactivity investigation of quinone-based dimeric cationic triazolium amphiphiles selective against resistant fungal and bacterial pathogens. *Eur. J. Med. Chem. 126*, 696−704.
(36) Shrestha, J. P., Subedi, Y. P., Chen, L. L., and Chang, C.-W. T. (2015) *MedChemComm 6*, 2012−2022.
(37) Davis, T. D., Gerry, C. J., and Tan, D. S. (2014) General platform for systematic quantitative evaluation of small-molecule permeability in bacteria. *ACS Chem. Biol. 9* (11), 2535−2544.
(38) Haldar, S., and Karmakar, K. (2015) A systematic understanding of gelation self-assembly: solvophobically assisted supramolecular gelation via conformational reorientation across amide functionality on a hydrophobically modulated dipeptide based ambidextrous gelator, N-n-acyl-(L)Val-X(OBn), (X = 1,ω-amino acid). *RSC Adv. 5* (81), 66339−66354.
(39) Ryu, H., Baek, J. H., Choi, M. G., Lee, J. C., and Chang, S.-K. (2017) Cu 2+-selective turn-on fluorescence signaling based on metal-induced hydrolysis of pyrenecarbohydrazide. *Tetrahedron Lett. 58* (30), 2927−2930.
(40) Gao, J., Wang, P., and Giese, R. W. (2002) (2002) Xanthamide fluorescent dyes. *Anal. Chem. 74* (24), 6397−6401.
(41) CLSI (2002) *Reference method for broth dilution antifungal susceptibility testing of yeasts; approved standard*, 2nd ed., Document M27-A2, CLSI, Wayne, PA, USA.
(42) CLSI (2008) *Reference method for broth dilution antifungal susceptibility testing of filamentous fungi; approved standard*, 2nd ed., Document M38-A2, CLSI, Wayne, PA, USA.

DOI: 10.1021/acsinfecdis.8b00327
ACS Infect. Dis. 2019, 5, 473−483